Deconstructing protein and gene expression pathways to define the anticancer effects of XPO1 inhibition in ovarian cancer

Brad R. Evans[1], Thomas R. Silvers[1], Ying A. Chen[1], Jason Garcia[1], Catalina Camacho[1], Andrew J. Sharp[1], Paras Garag[1], Srinivas V. Koduru[2], Jean-Noel Billaud[3], Richard L. Halpert[3], Peter R. Dottino[1], Yosef Landesman[4], Sharon Shacham[4], John A. Martignetti[1].

[1]Department of Genetics and Genomics Sciences, Icahn School of Medicine at Mount Sinai, New York, NY; [2]Gene Arrays, New York, NY; [3]Qiagen Bioinformatics, Redwood City, CA; [4]Karyopharm Therapeutics Inc., Natick, MA

Abstract

Emerging evidence across multiple cancer types, including ovarian cancer (OvCa),[1] has identified disruption in nuclear-cytoplasmic shuttling with overexpression of exportin-1 (XPO1), a key regulator of nuclear transport, as being linked to cancer aggressiveness, chemoresistance, and decreased patient survival.[2,3,4,5,6] These findings and that XPO1 is the sole transporter of a number of tumor suppressors and cell cycle regulators including TP53, BRCA1, CDKN1A, CDKN1B and FOXO, establishes the rationale for targeted therapeutic inhibition of XPO1.[7,8] KPT-185 and KPT-330 (generic name: selinexor) are two Selective Inhibitors of Nuclear Export (SINE) that inhibit XPO1. KPT-330/ selinexor is currently in multiple phase I clinical trials for both solid and hematologic cancers.[9,10]

We now demonstrate that despite similar XPO1 expression levels, patient-derived OvCa cell lines (PD-OvCa)[12] exhibit a broad differential IC50 response to SINE. To define the mechanism(s) of action underlying sensitivity and resistance and better understand the role of defective nuclear:cytoplasmic shuttling in OvCa, we examined the global differences between pathway activation/inhibition following XPO1 inhibition using nuclear:cytoplasmic fractionated protein lysates (reverse phase protein arrays, RPPA) and genome-wide RNA expression analysis using an Illumina-based high density microarray in three OvCa cell lines, OVCAR-3, A2780 and CP70.

Treatment of differentially sensitive OvCa lines resulted in nuclear accumulation of XPO1 and multiple known XPO1 cargo proteins including TP53 and CDKN1A, with a subsequent decrease in cytoplasmic XPO1 levels. RPPA analysis (MD Anderson RPPA Core) was then used to simultaneously examine the expression and subcellular localization of >200 proteins involved in a variety of biological and cancer-relevant processes. Numerous proteins accumulated in the nucleus including several known XPO1 cargoes, TP53 and YWHAZ, whereas a number of oncoproteins had decreased nuclear levels including MYC and RELA. These findings were shared across multiple OvCa lines. However, and as would be expected based on different cell contexts, many of the proteins had differential accumulation patterns between cell lines. The effects of these changes on the transcriptome were defined by microarray analysis (Illumina, HumanHT12, v4 Expression BeadChip). Ingenuity Pathway Analysis (IPA) revealed multiple shared pathways activated by XPO1 inhibition between OvCa lines (TP53, FOXO3, EPAS1, MITF, and MYOD1) and these were consistent with the RPPA data. However, multiple pathways, both activated and inhibited, did not overlap between OvCa lines and were thus unique to each cell line.

These data begin to reveal not only the multiple conserved pathways by which SINE effect their anticancer activity but also that, depending on cell context, these pathways can differ and may not overlap completely. The pathways and their more complete investigation defining their effect on differential sensitivity to XPO1 inhibition and their role in OvCa will be discussed.

Methods

•Patient samples were collected per our IRB and PD-OvCa cell lines were isolated and established as described by X. Liu, et al (2012). *J Path* **180**(2):599-607.
•MTTs were performed to establish relative sensitivity to KPT-185 between PD-OvCa lines.
•Total RNA and whole cell lyates were isolated from PD-OvCa cell lines and used to measure mRNA expression of XPO1 by real-time PCR (RT-PCR) and XPO1 protein expression via western blot analysis, respectively.
•OVCAR-3 cells were treated with KPT-185, IC50 [116.1 nM], for varying time points and cells were collected and fractionated into cytoplasmic and nuclear lysate fractions. Western blot analysis of known XPO1 cargoes was performed to determine earliest time point of maximal protein accumulation in the nucleus upon XPO1 inhibition.
•OVCAR-3, A2780 and CP70 cells were dosed with their individual IC50 of KPT185 ([116.1 nM], [46.5 nM], [111.7 nM], respectively) for 6 hours and nuclear fractions were collected and sent to the MD Anderson RPPA core for RPPA analysis.
•Fold change (FC) relative to control from the RPPA analysis for each cell line was calculated following variance stabilization normalization.
•Select proteins FC was verified via western blot analysis.
•OVCAR-3 cells were treated with KPT-185, [IC50], for varying time points and total RNA was collected and RT-PCR was performed with genes that are downstream of the known XPO1 cargoes used in the temporal western blot experiment.
•OVCAR-3, A2780 and CP70 cells were dosed with KPT185, [IC50], for 9 hours and total RNA was collected and used for microarray analysis using the Illumina, HumanHT12, v4 Expression BeadChip at the Genomics Core at the Icahn School of Medicine at Mount Sinai. Expression data was scanned through Illumina's Genome Studio Software normalizing data with internal standards (n=3).
•Microarray data was analyzed using Genespring GX 12.5 platform (1), raw data was normalized and applied test to compare gene expression between experimental groups using the median of control samples with multiple test corrections (Benjamini and Hochberg FDR).
•RT-PCR was used to confirm the relative FC of select genes.
•Ingenuity IPA analysis™ was performed on microarray data where the absolute FC≥1.5 and the p-value≤0.05 to determine Upstream Regulators (URs) of signaling pathways. URs were determined from changes in the expression of a set of genes defined by IPA and having a Activated Z-score ≥ 2. This genetic signature has been defined by IPA to correlate the expression pattern of genes with activation or inhibition of UR.
•Western blot analysis was performed to validate select Ingenuity IPA analysis™ of changes in UR signaling pathways.

Results

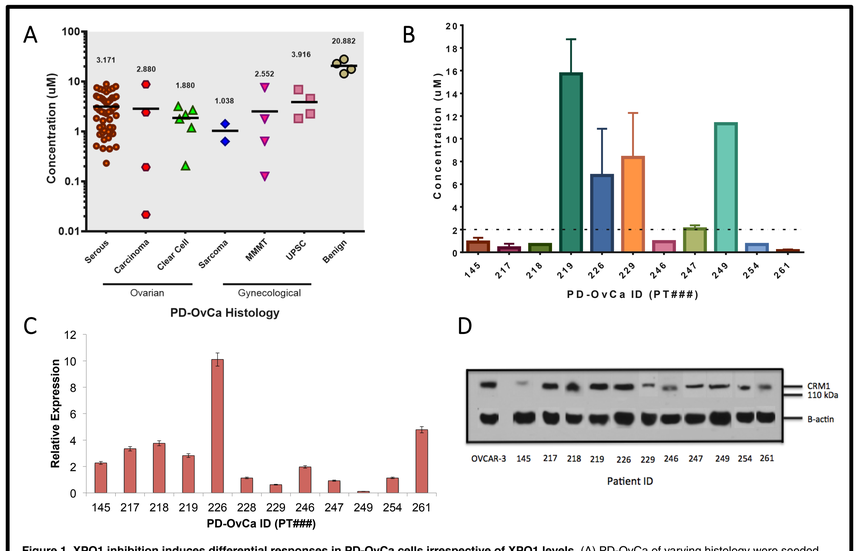

Figure 1. XPO1 inhibition induces differential responses in PD-OvCa cells irrespective of XPO1 levels. (A) PD-OvCa of varying histology were seeded in 96-well plates and treated with KPT-185 for 48 h at a concentration range of 0.01 to 40 uM. PD cell lines established from additional gynecologic cancers are also shown Cell viability was measured by MTT assay. Each point represents a unique cell line experiment. Numbers are the average IC50. (B) KPT-185 IC50s of individual PD-OvCas from MTTs. Dotted horizontal line corresponds to 2 uM concentration; levels above this are consistent with patient resistance to KPT. (*n*=3, except where noted). (C) Real-time PCR analysis of XPO1 mRNA expression from individual PD-OvCas relative to OVCAR-3 (*n*=2). (D) Representative Western blot analysis of XPO1 protein expression using individual PD-OvCa (*n*=3).

References

1. S.L. Cooke , J.D. Brenton (2011). *The Lancet Oncology* **12**, 1169-1174.
2. G.L. Gravina, et al (2014). *J of Hemat & Oncol* **7**, 85-93.
3. K.M. Brodie, B.R. Henderson (2012) *J Biol Chem* **12**;287:7701-7716.
4. A. Noske, et al (2008). *Cancer* **112**, 1733-1743.
5. Y. Wang Y, et al (2013). *Cancer Letters* **343**, 6-13.
6. E.S. Newlands, et al (1996). *Br. J. Cancer* **74**, 648-9.
7. B.R. Henderson, A. Eleftheriou. (2000). *Exp Cell Res* **256**: 213-224.
8. X Han, et al (2008). *Oncogene* **27**, 2969-2977.
9. Y.T. Tai, et al (2014). *Leukemia* **28**(1):155-65.
10. J. Yang, et al (2014) . *PLoS One* **9**, e102983.
11. J.A. Martignetti, et al (2014). *J Clin Oncol* **32**, abstr 5522.
12. X. Liu, et al (2012). *J Path* **180**(2):599-607.

Results

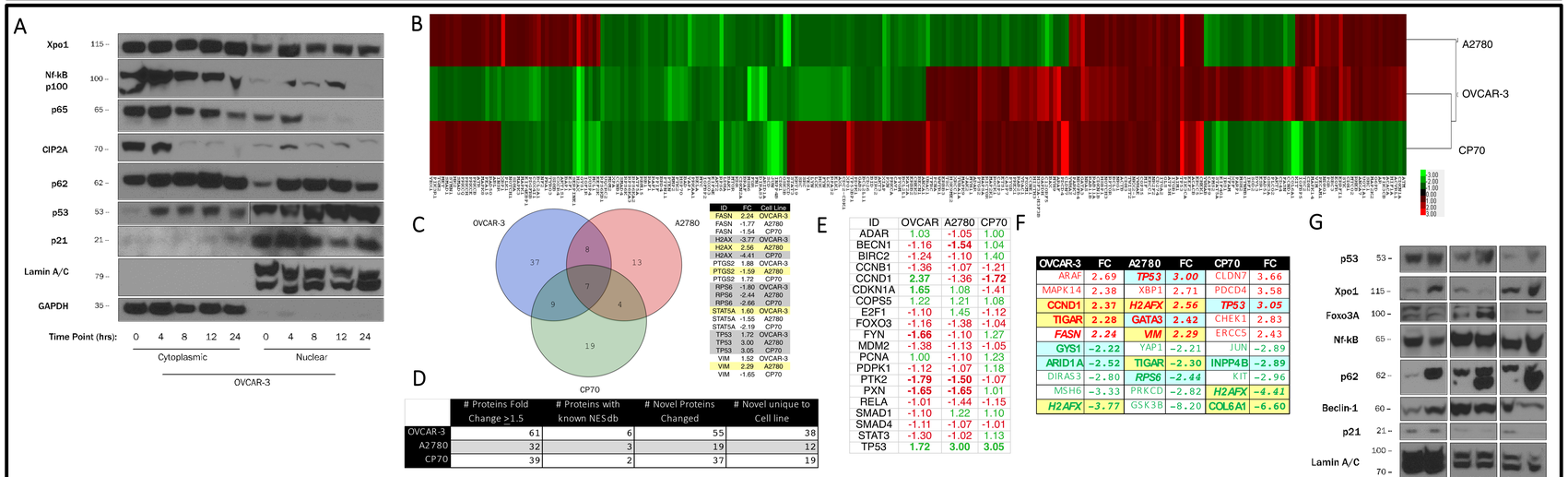

ID	FC	Cell Line
FASN	2.24	OVCAR-3
FASN	-1.77	A2780
FASN	-1.54	CP70
H2AX	-3.77	OVCAR-3
H2AX	2.56	A2780
H2AX	-4.41	CP70
PTGS2	1.88	OVCAR-3
PTGS2	-1.59	A2780
PTGS2	1.72	CP70
RPS6	-1.80	OVCAR-3
RPS6	-2.44	A2780
RPS6	-2.66	CP70
STAT5A	1.60	OVCAR-3
STAT5A	-1.55	A2780
STAT5A	-2.19	CP70
TP53	1.72	OVCAR-3
TP53	3.00	A2780
TP53	3.05	CP70
VIM	1.52	OVCAR-3
VIM	2.29	A2780
VIM	-1.65	CP70

	# Proteins Fold Change >1.5	# Proteins with known NESdb	# Novel Proteins Changed	# Novel unique to Cell line
OVCAR-3	61	6	55	38
A2780	32	3	19	12
CP70	39	2	37	19

ID	OVCAR	A2780	CP70
ADAR	1.03	-1.05	1.00
BECN1	-1.16	**-1.54**	1.04
BIRC2	-1.24	-1.10	1.40
CCNB1	-1.36	-1.07	-1.25
CCND1	2.37	-1.36	**-1.72**
CDKN1A	1.65	1.08	-1.41
COPS5	1.22	1.21	1.08
E2F1	-1.10	1.45	-1.12
FOXO3	-1.16	-1.38	-1.04
FYN	**-1.66**	-1.10	1.27
MDM2	-1.38	-1.13	-1.05
PCNA	1.00	-1.10	1.23
PDPK1	-1.12	-1.07	1.18
PTK2	**-1.79**	**-1.50**	-1.07
PXN	**-1.65**	**-1.65**	1.01
RELA	-1.01	-1.44	-1.15
SMAD1	-1.10	1.22	1.10
SMAD4	-1.11	-1.07	-1.01
STAT3	-1.30	-1.02	1.13
TP53	**1.72**	**3.00**	**3.05**

OVCAR-3	FC	A2780	FC	CP70	FC
ARAF	2.69	*TP53*	***3.00***	CLDN7	3.66
MAPK14	2.38	XBP1	2.71	PDCD4	3.58
CCND1	**2.37**	***H2AFX***	***2.56***	***TP53***	***3.05***
TIGAR	**2.28**	**GATA3**	**2.42**	CHEK1	2.83
FASN	***2.24***	***VIM***	***2.29***	ERCC5	2.43
GYS1	-2.22	YAP1	-2.21	JUN	-2.89
ARID1A	-2.52	TIGAR	-2.30	INPP4B	-2.89
DIRAS3	-2.80	*RPS6*	***-2.44***	KIT	-2.96
MSH6	-3.33	PRKCD	-2.82	***H2AFX***	***-4.41***
H2AFX	***-3.77***	GSK3B	-8.20	**COL6A1**	**-6.60**

Figure 2. Differential nuclear protein accumulation pattern between OvCa cell lines following XPO1 inhibition. (**A**) Western blot analysis of OVCAR-3 nuclear fractionated lysates following treatment with KPT-185 (IC50 [116.1 nM]) at indicated time points. Targeted XPO1 protein export substrates were measured. (**B**) Heatmap of RPPA protein fold changes between KPT-185-treated and control cells in three OvCa cell lines (n=3). The fold change was calculated after variance stabilization normalization. Red indicates an increase in fold change; green indicates a decrease. The heatmap was generated in Cluster 3.0 (http://bonsai.hgc.jp/~mdehoon/software/cluster/software.htm) as a hierarchical cluster using Pearson correlation and a center metric and was visualized in Treeview (http://rana.lbl.gov/EisenSoftware.htm). (**C**) Venn diagram of number of overlapping proteins with an absolute fold change of 1.5 in KPT-185-treated cell lines. Table of 7 proteins found in all cell lines with cel line in disagreement highlighted. (**D**) Relative fold change of proteins from RPPA analysis with a known XPO1 NES. Proteins in the RPPA analysis were compared to the NESdb (http://prodata.swmed.edu/LRNes/IndexFiles/names.php). (**E**) Table of number of proteins with an absolute fold change of 1.5 and NES status. Red indicates an increase and green indicates a decrease in fold change of KPT-185 treated cells vs. controls. (**F**) Table of top 10 proteins with highest resultant fold change from each cell line. Red indicates an increase and green indicates a decrease in fold change of KPT-185 treated cells vs. controls. **Bold** proteins appear in 2 cell lines, while Italics proteins appear in all 3 cells lines. (**G**) Confirmation of key candidate proteins with known NES by western blot.

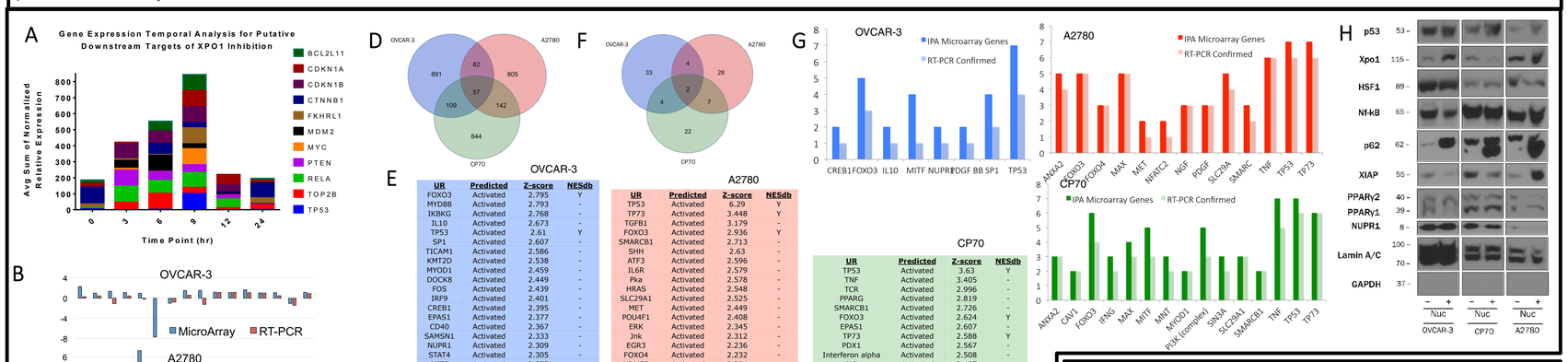

UR	Predicted	Z-score	NESdb
FOXO3	Activated	2.795	Y
MYD88	Activated	2.793	-
IKBKG	Activated	2.768	-
IL10	Activated	2.673	-
TP53	Activated	2.61	Y
SP1	Activated	2.607	-
TICAM1	Activated	2.586	-
KMT2D	Activated	2.538	-
MYOD1	Activated	2.459	-
DOCK8	Activated	2.449	-
FOS	Activated	2.439	-
IRF9	Activated	2.401	-
CREB1	Activated	2.395	-
EPAS1	Activated	2.377	-
CD40	Activated	2.367	-
SAMSN1	Activated	2.333	-
NUPR1	Activated	2.309	-
STAT4	Activated	2.305	-
MITF	Activated	2.275	-
Cg	Activated	2.253	-
MAVS	Activated	2.236	-
IL5	Activated	2.22	-
CCL5	Activated	2.219	-
NGF	Activated	2.214	-
FOXO1	Activated	2.21	-
CAV1	Activated	2.208	-
TBK1	Activated	2.208	-
PDGF BB	Activated	2.128	-
NFATC2	Activated	2.121	-
F2	Activated	2.11	-
VIP	Activated	2.095	-
CTNNB1	Activated	2.086	-
GDF2	Activated	2.061	-
DDX58	Activated	2	-
HOXC8	Activated	2	-
UBE2I	Activated	2	-
ACKR2	Inhibited	-2	-
Irgm1	Inhibited	-2	-
MGEA5	Inhibited	-2	-
FGF1	Inhibited	-2.111	-
KLF2	Inhibited	-2.387	-
SATB1	Inhibited	-2.395	-
IRF8	Inhibited	-2.557	-

UR	Predicted	Z-score	NESdb
TP53	Activated	6.29	Y
TP73	Activated	3.448	Y
TGFB1	Activated	3.179	-
FOXO3	Activated	2.936	Y
SMARCB1	Activated	2.713	-
SHH	Activated	2.63	-
ATF3	Activated	2.596	-
IL6R	Activated	2.579	-
Pka	Activated	2.578	-
HRAS	Activated	2.548	-
SLC29A1	Activated	2.525	-
MET	Activated	2.449	-
POU4F1	Activated	2.408	-
ERK	Activated	2.345	-
Jnk	Activated	2.312	-
EGR3	Activated	2.236	-
FOXO4	Activated	2.232	-
KDM5B	Activated	2.224	-
PDGF BB	Activated	2.224	-
NGF	Activated	2.213	-
BMP6	Activated	2.19	-
Smad	Activated	2.187	-
NFATC2	Activated	2.173	-
DCN	Activated	2.164	-
HIPK2	Activated	2.159	-
NRG1	Activated	2.157	-
MAP3K8	Activated	2.121	-
TP63	Activated	2.051	-
WNT3A	Activated	2.045	-
TNF	Activated	2.029	-
CREBBP	Activated	2.023	-
BTNL2	Activated	2	-
SAMSN1	Activated	2	-
SMAD2	Activated	2	-
SQSTM1	Activated	2	-
FOXA2	Inhibited	-2.183	Y
MAX	Inhibited	-2.213	-
HNF1A	Inhibited	-2.36	-
PITX2	Inhibited	-2.372	-
AHR	Inhibited	-2.416	Y
NOG	Inhibited	-2.433	-
ANXA2	Inhibited	-2.728	-

UR	Predicted	Z-score	NESdb
TP53	Activated	3.63	Y
TNF	Activated	3.405	-
TCR	Activated	2.996	-
PPARG	Activated	2.819	-
SMARCB1	Activated	2.726	-
FOXO3	Activated	2.624	Y
EPAS1	Activated	2.607	-
TP73	Activated	2.588	Y
PDX1	Activated	2.567	-
Interferon alpha	Activated	2.508	-
IL3	Activated	2.465	-
BTNL2	Activated	2.449	-
HIC1	Activated	2.449	-
MYOD1	Activated	2.35	-
P38 MAPK	Activated	2.277	-
IFN Beta	Activated	2.236	-
NFkB (complex)	Activated	2.203	-
NFKB1	Activated	2.157	-
SLC29A1	Activated	2.121	-
ESR2	Activated	2.101	-
CAV1	Activated	2.072	-
MITF	Activated	2.021	-
IFNG	Activated	2.019	-
BNIP3L	Activated	2	-
RPS6KB1	Activated	2	-
HGF	Inhibited	-2.095	-
E2F2	Inhibited	-2.2	-
EP400	Inhibited	-2.4	-
MNT	Inhibited	-2.449	-
SIN3A	Inhibited	-2.449	-
ANXA2	Inhibited	-2.63	-
PI3K (complex)	Inhibited	-2.667	-
FSH	Inhibited	-2.781	-
MAX	Inhibited	-2.813	-
Lh	Inhibited	-3.11	-

Cell Line Tx	# Genes	Total # URs	Activated # URs	Inhibited # URs
OVCAR-3	1139	43	36	7
A2780	1086	42	35	7
CP70	1152	38	28	10

Figure 3. Transcriptome analysis identifies unique upstream regulators of signaling pathways activated/inhibited following XPO1 inhibition. (**A**) RT-PCR measurement of downstream gene targets of XPO1 cargoes from Figure 2A following treatment of OVCAR-3 cells with (IC50 [116.1 nM]) for varying time points. Relative gene expression was calculated through normalization of data on a percentage scale based on highest expression level. Cumulative relative expression of all measured genes was combined to determine maximal cumulative relative expression point (n=2). (**B**) Confirmation of relative fold change between KPT-treated cells versus control microarray data using real-time PCR. RT-PCR primers were designed and RT-PCR was performed and relative fold change between KPT-185 treated and control cells was calculated (n=2). (**C**) Number of genes from each cell line that had an absolute fold change ≥1.5 and a p-value≤0.05 that were used for subsequent Ingenuity IPA analysis™. Number of upstream regulators of signaling pathways (URs) identified by IPA analysis of microarray data. Table indicates 7 overlapping proteins between all three cell lines. (**D**) Venn diagram showing overlapping genes used in IPA analysis between OvCa cell lines. (**E**) Putative "Upstream Regulators" (UR) derived from IPA analysis of microarray data. Activation stated, calculated Z-score, and known NES are indicated. (**F**) Venn diagram showing overlap between UR between OvCa cell lines. (**G**) RT-PCR confirmation of UR gene signatures. The number of genes taken from the IPA analysis measured in the microarray to identify URs was compared to the RT-PCR expression to determine the number of genes in agreement. (**H**) Western blot analysis of nuclear fractionated lysates of OvCa cell lines of a subset of URs to confirm IPA analysis of activation of signaling pathway.

Figure 5. Model of XPO1 inhibition mechanism of action in ovarian cancer cell lines.

Cell Line	Upstream Regulator	Predicted Activation State	Activation Z-score	RPPA Fold Change
OVCAR-3	CAV1	**Activated**	**2.208**	**-1.2466**
	CTNNB1	**Activated**	**2.086**	**1.3273**
	FOXO3	**Activated**	**2.795**	**-1.1589**
	TP53	**Activated**	**2.61**	**1.7152**
A2780	ERK	**Activated**	**2.345**	**1.0107**
	FOXO3	**Activated**	**2.936**	**-1.3782**
	Jnk	**Activated**	**2.312**	**1.1896**
	MET	**Activated**	**2.449**	**1.0639**
	NRG1	**Activated**	**2.157**	**1.0658**
	Smad	**Activated**	**2.187**	**1.2244**
	TP53	**Activated**	**6.29**	**2.9995**
CP70	CAV1	**Activated**	**2.072**	**1.0848**
	FOXO3	**Activated**	**2.624**	**-1.0403**
	NFkB	**Activated**	**2.203**	**-1.1512**
	P38 MAPK	**Activated**	**2.277**	**-1.1132**
	RPS6KB1	**Activated**	**2**	**-1.3285**
	TP53	**Activated**	**3.63**	**3.0464**

Figure 4. Correlation of predicted URs with RPPA expression. (**A**) Activation state of predicted URs from IPA analysis of microarray data with corresponding fold changes of the protein levels in the RPPA analysis. (**B**) RT-PCR of UR gene signatures as described above in Figure 3G. (**C**) Western blot analysis of nuclear fraction lysates confirms correlation of UR/RPPA expression levels from cells treated with KPT-185.

Conclusions & Future Directions

- PD-OvCa and OvCa cell lines exhibit a differential sensitivity to XPO1 inhibition by KPT-185.
- XPO1 inhibition results in a unique proteomic and transcriptional profile between the three OvCa cell lines examined.
- Ingenuity IPA analysis allowed for identification of potential URs that were validated by RPPA analysis.
- Discrepancies between RPPA analysis and URs from microarray analysis indicate the importance of doing distinct and overlapping techniques to elucidate the relevant proteins and genes responsible for the antitumor effects of XPO1 inhibition.
- There are overlapping proteins and URs that could be the "select cargoes" (i.e TP53, CAV1, RPS6, etc.) that may be responsible for the antitumor effects of XPO1 inhibition by KPT-185.
- The unique URs and proteins affected by XPO1 inhibition in each cell line may result in similar/parallel pathways leading to cellular death and a decrease cell proliferation.
- Further explore proteins with a FC>1.5 common to all three cell lines.
- Examine other URs to confirm activation/inhibition in more depth by pathway analysis rankings of relevance.
- Validate the RPPA expression of Urs to confirm status.
- Identify proteins from RPPA and URs that could contribute to decreased cellular proliferation and increased cell death.